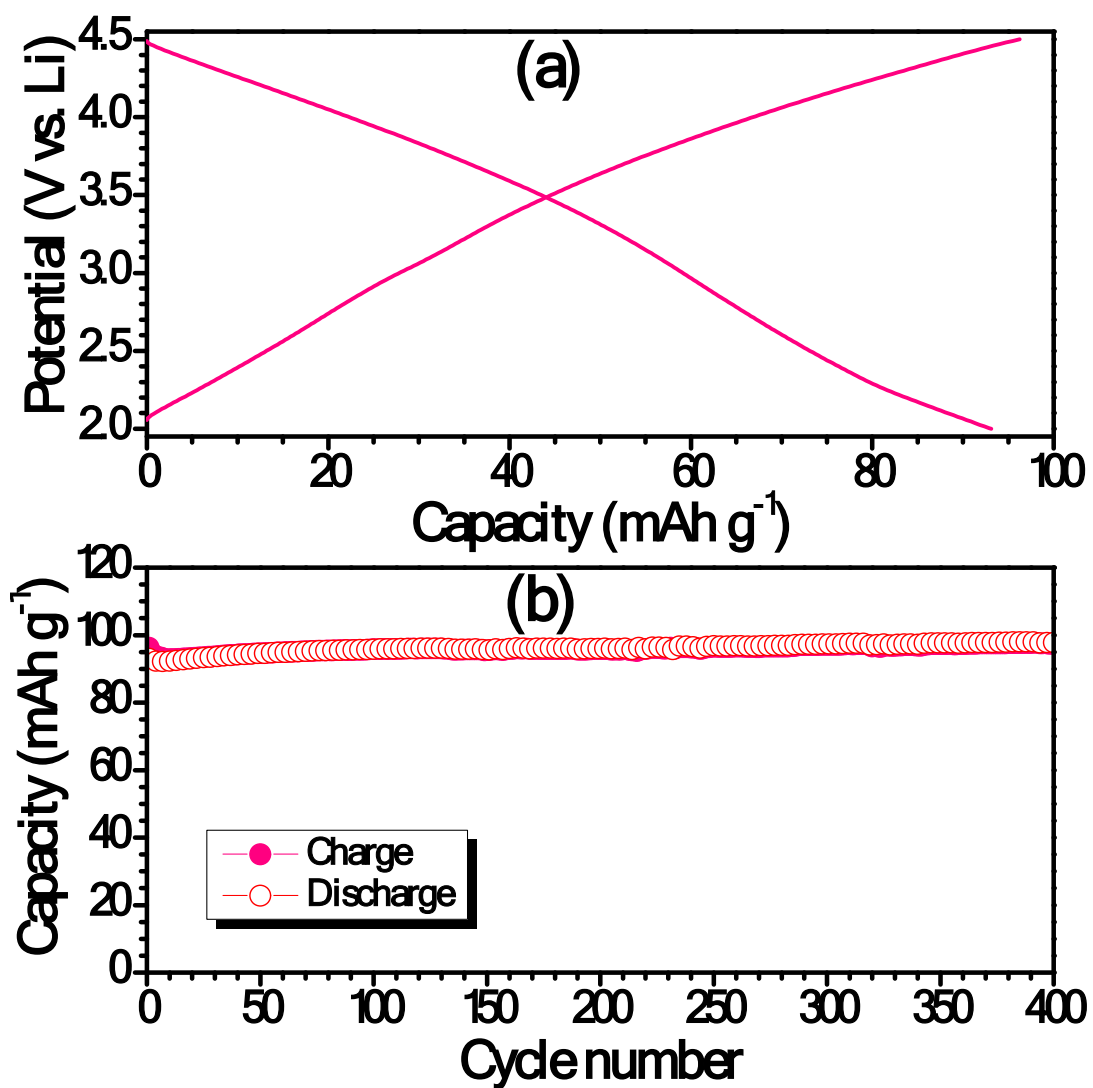
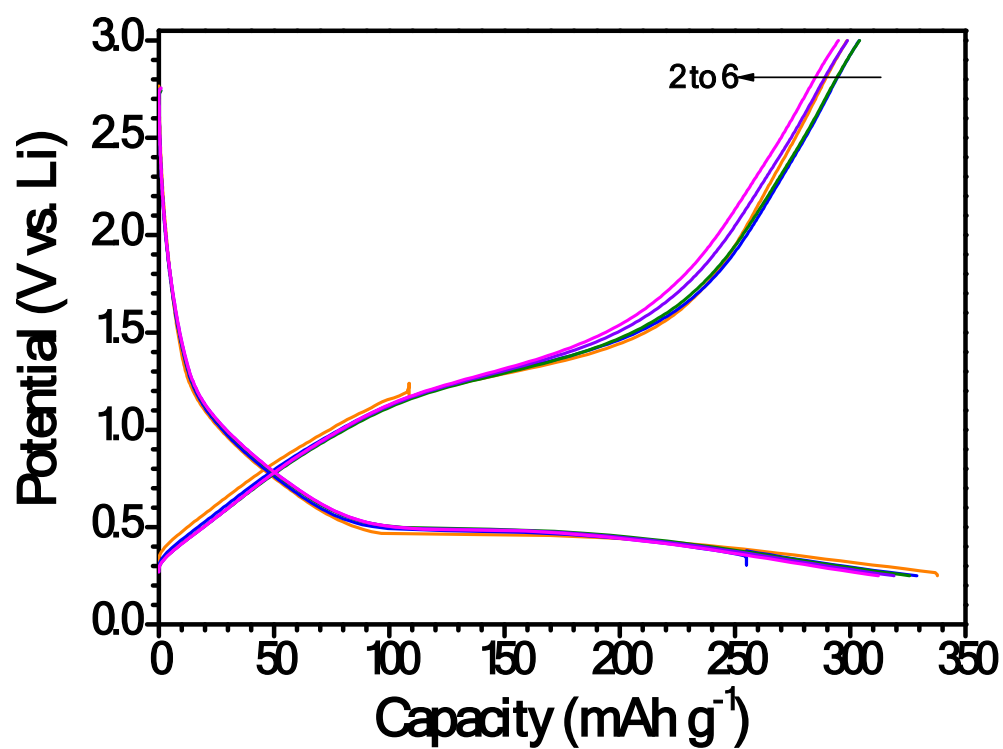


Supplementary information



**Figure S1.** (a) Galvanostatic charge-discharge curves of AC (Kuraray, Japan) in half-cell configuration with Li at current density of 100 mA g<sup>-1</sup>, and (b) Plot of capacity vs. cycle number



**Figure S2.** Typical galvanostatic charge-discharge curves of Mn<sub>3</sub>O<sub>4</sub>-G in half-cell configuration with Li at current density of 100 mA g<sup>-1</sup>.

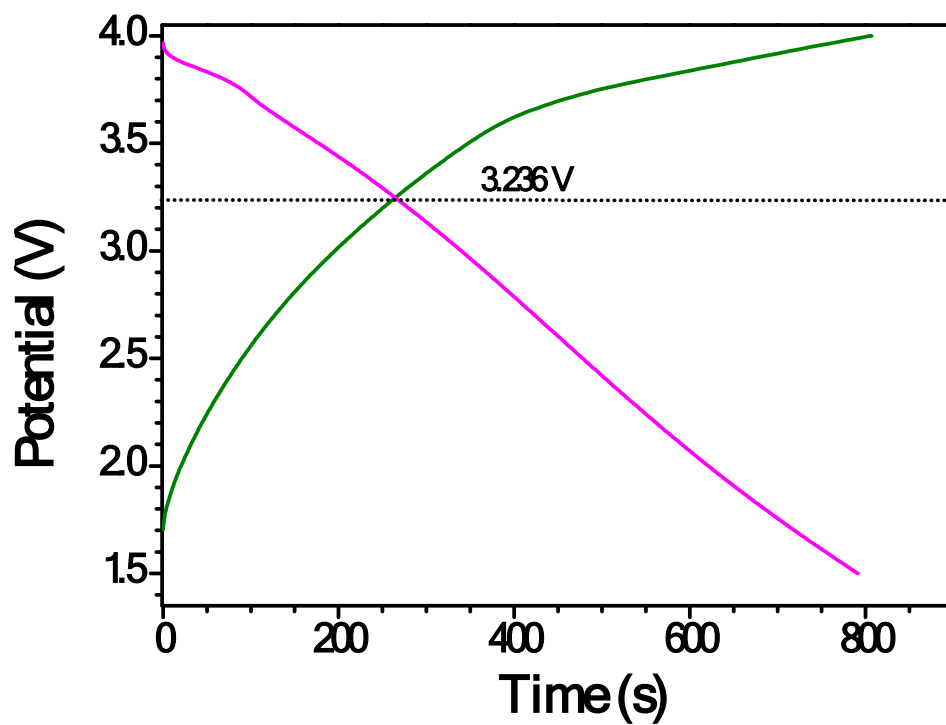


**Figure S3.** Typical charge-discharge curves of AC/Mn<sub>3</sub>O<sub>4</sub>-G based LIC at current density of 0.2 A g<sup>-1</sup>

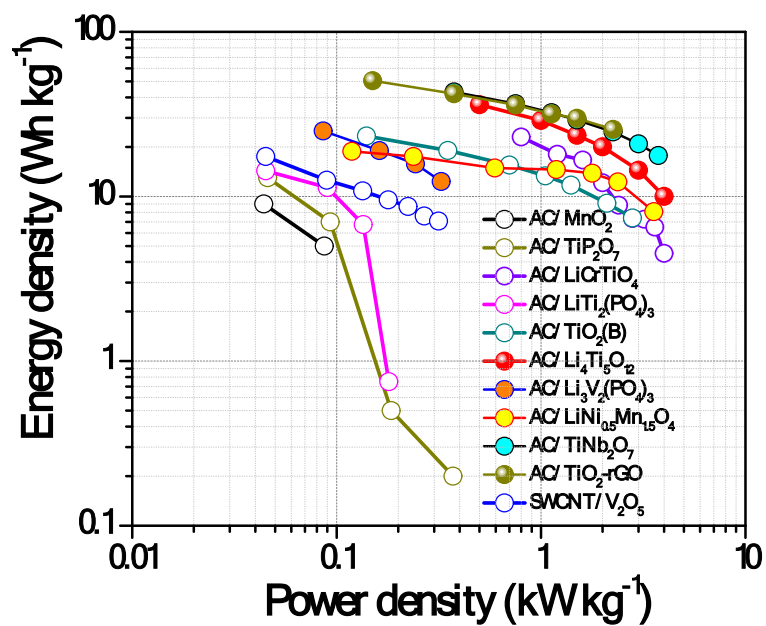


**Figure S4.** Ragone plot of various insertion type material investigated for LIC perspective. The given values are based on the total mass of the active material.

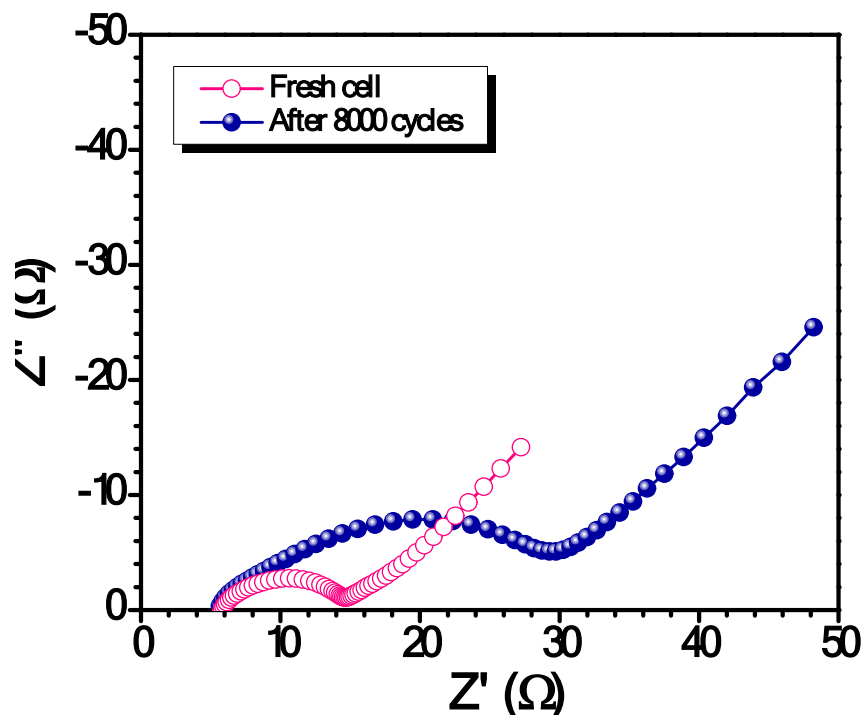


**Figure S5.** Electrochemical impedance spectra of AC/Mn<sub>3</sub>O<sub>4</sub>-G based LIC

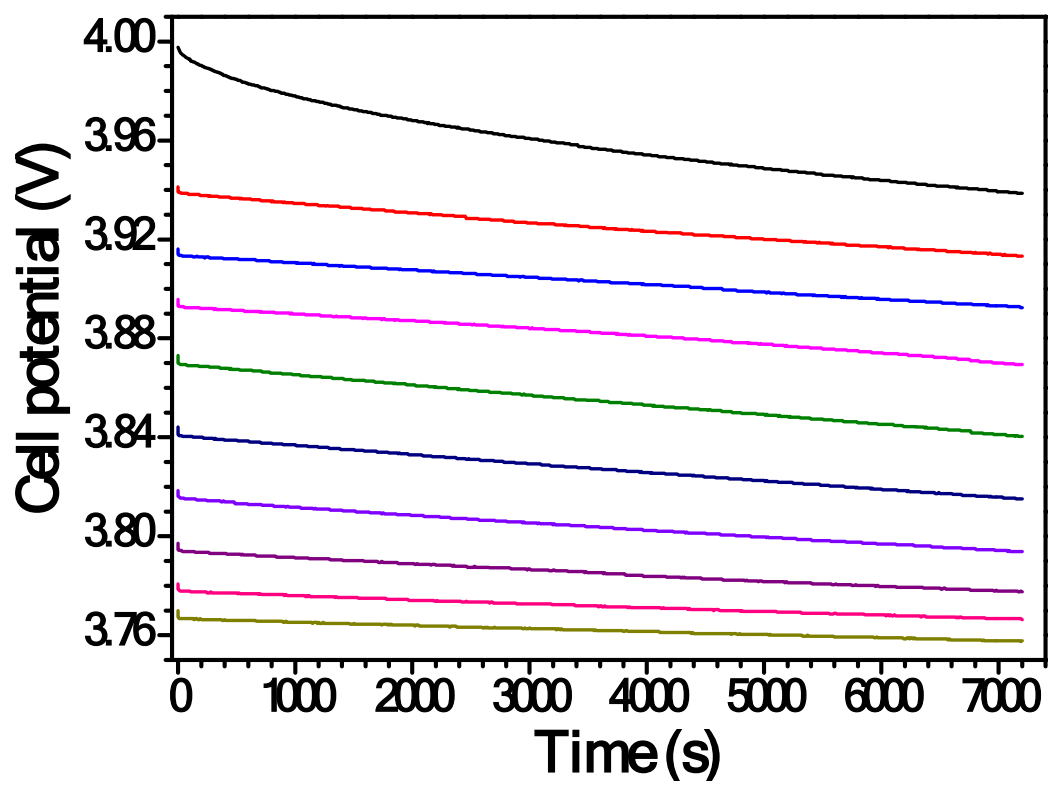


**Figure S6.** Plot of cell potential vs. relaxation time for AC/Mn<sub>3</sub>O<sub>4</sub>-G based LIC towards self-discharge measurements.

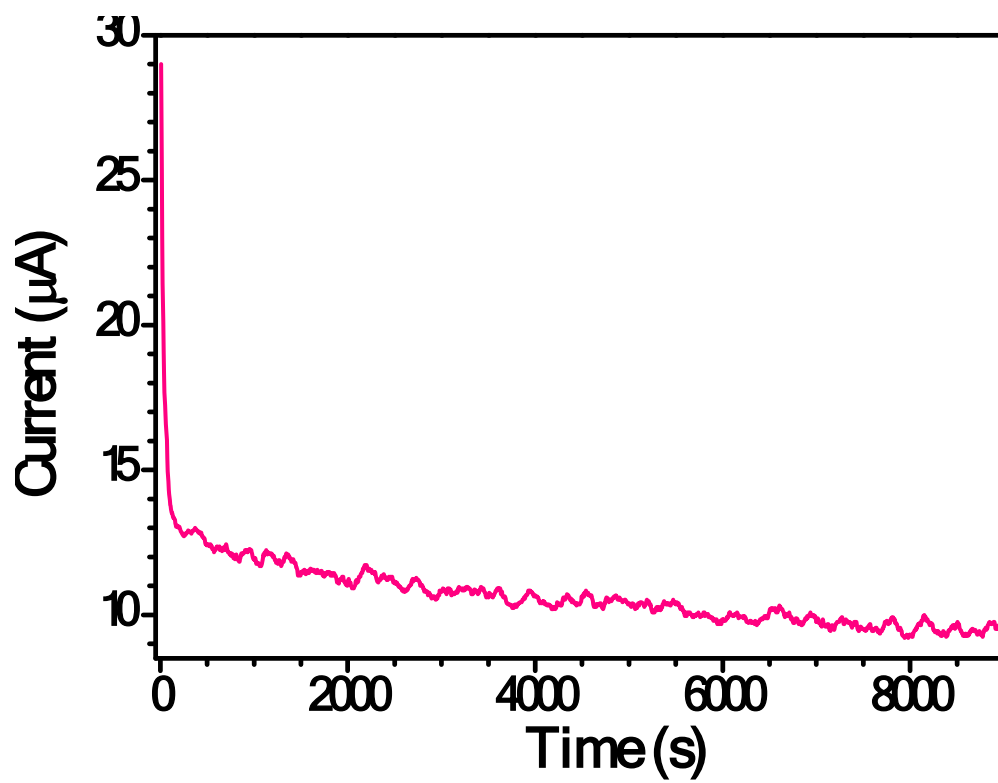


**Figure S7.** Plot of leakage current vs. time when the AC/Mn<sub>3</sub>O<sub>4</sub>-G based LIC is at 4 V.

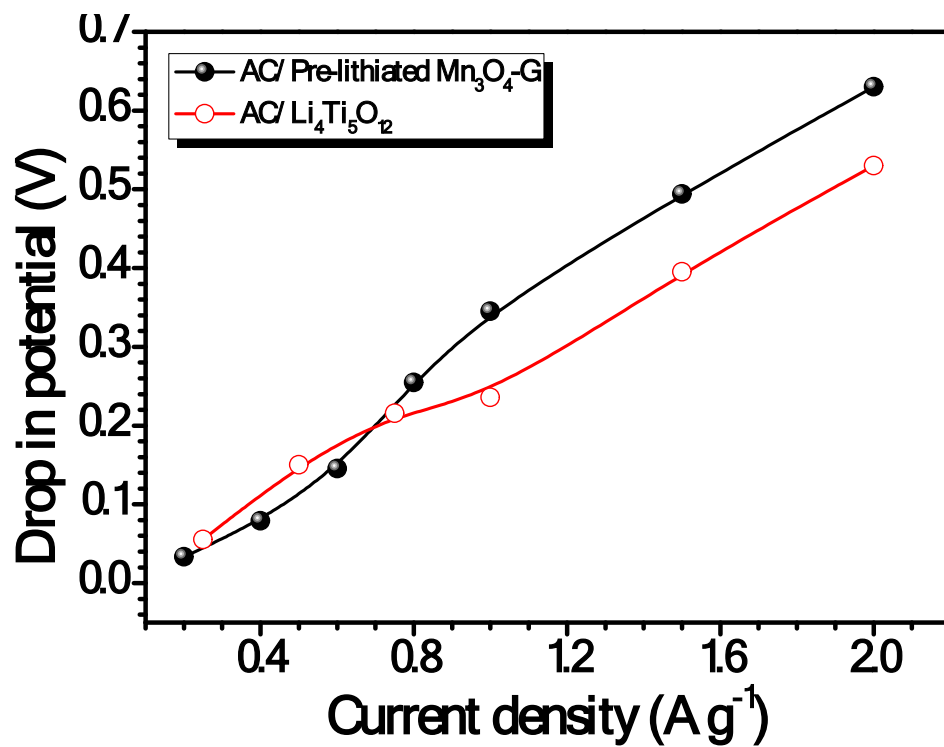


**Figure S8.** Comparison of IR drop observed in this system with intercalation anode based LIC (AC/Li<sub>4</sub>Ti<sub>5</sub>O<sub>12</sub>, Ref. 18)